MASTER COPY *KEEP THIS COPY FOR REPRODUCTION PURPOSES

REPORT DOCUMENTATION PAGE

Form Approved
OMB No. 0704-0188

1. AGENCY USE ONLY (Leave blank)	2. REPORT DATE	3. REPORT TYPE AND DATES COVERED
	September 1997	Final Report 9-20-94 - 6-30-97

4. TITLE AND SUBTITLE
Affordable Optoelectronic Module Technology

5. FUNDING NUMBERS
DAAH04-94-C-0049

6. AUTHOR(S)
Michael A. Haase

7. PERFORMING ORGANIZATION NAME(S) AND ADDRESS(ES)
Minnesota Mining & Manufacturing (3M Company)
Bldg. 201-1N-35, 3M Center
St. Paul, MN 55144-1000

8. PERFORMING ORGANIZATION REPORT NUMBER

9. SPONSORING / MONITORING AGENCY NAME(S) AND ADDRESS(ES)
U.S. Army Research Office
P. O. Box 12211
Research Triangle Park, NC 27709-2211

10. SPONSORING / MONITORING AGENCY REPORT NUMBER
ARO 33787.1-PH

11. SUPPLEMENTARY NOTES
The views, opinions and/or findings contained in this report are those of the author(s) and should not be construed as an official Department of the Army position, policy, or decision, unless so designated by other documentation.

12a. DISTRIBUTION / AVAILABILITY STATEMENT
Approved for public release; distribution unlimited.

12b. DISTRIBUTION CODE

13. ABSTRACT (Maximum 200 words)

Blue-green laser diodes fabricated from II-VI compound semiconductors are developed for optical data storage applications. These lasers operate at wavelengths between 460 and 540nm. Both sulfur-based and beryllium-based alloys are demonstrated. Dramatic improvements in material quality have led to significant improvements in device performance and reliability.

14. SUBJECT TERMS
blue-green laser diodes, optical data storage system

15. NUMBER OF PAGES
33

16. PRICE CODE

17. SECURITY CLASSIFICATION OF REPORT	18. SECURITY CLASSIFICATION OF THIS PAGE	19. SECURITY CLASSIFICATION OF ABSTRACT	20. LIMITATION OF ABSTRACT
UNCLASSIFIED	UNCLASSIFIED	UNCLASSIFIED	UL

ARO FINAL TECHNICAL REPORT

Title of Proposal: Affordable Optoelectronic Module Technology

Author of Report: Michael A. Haase

Period Covered by Report: September 20, 1994 - June 30, 1997

ARO Proposal Number: 33787-PH

Contract or Grant Number: DAAH04-94-C-0049

Name of Institution: Minnesota Mining & Manufacturing (3M Company)

Approved for Public Release;
Distribution Unlimited

Abstract

Blue-green laser diodes fabricated from II-VI compound semiconductors are developed for optical data storage applications. These lasers operate at wavelengths between 460 and 540 nm. Both sulfur-based and beryllium-based alloys are demonstrated. Dramatic improvements in material quality have led to significant improvements in device performance and reliability.

1. Introduction

Applications

Blue-green laser diodes are a key enabling technology for a number of important industries. At present, II-VI compound semiconductors (e.g., ZnSe) are the only semiconductor materials capable of generating laser light at these wavelengths (540 nm to 460 nm). The development of these devices is largely driven by the need for ever-higher information density in optical data storage. The area of the diffraction-limited laser spot on an optical recording medium is proportional to the square of the wavelength of the laser. If all other aspects of the system are equal, a shift from 780 nm infrared lasers to 500 nm blue-green lasers could provide a factor of 2.4 increase in information density. When combined with other new technologies, these laser promise to drive the coming generations of optical data storage products. This includes consumer products, such as DVD (Digital Video Disk).

Blue-green laser diodes will also find application in low cost, light weight, high brightness, high resolution projection displays made with laser diode arrays of AlGaInP (red), II-VI (green), and either II-VI or AlGaInN for blue.

Still other applications include a wide variety of sensors and laser surgery. Because the human eye is most sensitive to green wavelengths, these devices are attractive for applications such as laser pointers and laser weapon sights. Because sea water is more transparent to blue-green light than any other wavelength in the electromagnetic spectrum (including radio waves) these devices are also useful for undersea communications, mapping and fish location.

Historical Background

The first blue-green laser diodes were demonstrated at 3M in April of 1991[1]. Those separate confinement heterostructures devices featured CdZnSe quantum wells, ZnSe guiding layers, and ZnSSe cladding layers. The structure was grown by MBE on GaAs substrates and was demonstrated using pulsed current injection at cryogenic temperatures. Subsequent improvements in this technology included the development of MgZnSSe

[1] "Blue-green laser diodes," M.A. Haase, J. Qiu, J.M. DePuydt, and H. Cheng, Appl. Phys. Lett. **59,** 1272 (1991).

cladding layers and ZnSe-ZnTe graded contacts. Consequently, room temperature cw operation was first demonstrated in June of 1993[2].

This research program consisted of a collaboration between 3M Company and Philips Laboratories to develop and evaluate II-VI laser diodes for optical data storage applications. At the beginning of the program (September, 1994), the team had already demonstrated room temperature pulsed lasers that operated at wavelengths around 515 nm. These were based on CdZnSe/ZnSSe/MgZnSSe separate confinement heterostructures using ZnSe-ZnTe digitally graded *p*-type ohmic contacts. However, if operated at 10% duty factor these early devices lasted for only a few seconds before failing.

Among the technical issues facing this technology in 1994 were epitaxial crystal defects, *p*-type ohmic contacts, *p*-type doping at large band gaps, and device processing.

Crystallographic Defects

At the start of this program, the epitaxial layers (grown by molecular beam epitaxy, MBE, on GaAs substrates) typically had many extended crystallographic defects, such as stacking faults and dislocations. Typical defect densities ranged from 10^5 to 10^7 defects/cm^2. Defect densities of 10^3 cm^{-2} or less will be needed for production with good yield. The challenge was to achieve greatly improved control of the MBE process.

P-type Ohmic Contacts

A second challenge involved the electrical contacts to the p-type II-VI semiconductors. This had become a classical problem in these wide band gap materials. Although the use of ZnSe-ZnTe digitally graded contacts had reduced the laser operating voltage from greater than 20 V to about 9 V, the technology was immature and the resultant contacts were not reproducible. In addition, the contacts would degrade during operation, increasing the operating voltage of the laser.

P-type Doping

The preferred method of making p-type II-VI semiconductors was (and still is) the use of a plasma source to generate nitrogen free radical dopants during MBE[3]. Our experience suggested that this technique works for *p*-type doping of materials with band gaps less than about 2.8 eV . However, there was evidence that the doping efficiency decreases as the bandgap nears and exceeds 3 eV. This limit could define the lower limit of wavelengths that can be generated by II-VI laser diodes.

---

[2] "Room temperature continuous operation of blue-green laser didoes", N. Nakayama, S. Itoh, T. Ohata, K. Nakano, H. Okuyama, M. Ozawa, A. Ishibashi, M. Ikeda, and Y. Mori, Electronics Letters 29, 1488 (1993).

[3] "*p*-type ZnSe by nitrogen atom beam doping during molecular beam epitaxial growth," R.M. Park, M.B. Troffer, C.M. Rouleau, J.M. DePuydt, and M.A. Haase, Appl. Phys. Lett. **57**, 2127 (1990).

Device Fabrication

3M had already developed rudimentary index-guided laser fabrication processes that provided single transverse optical modes. The need was to evaluate the impact of processing on device reliability and to more fully characterize the optical performance of the devices.

Technical Results Summary

In proposing this research, a number of ambitious technical goals were proposed by the technical team to try to achieve in two years. Those targets, along with the actual results are presented in Table I.

	wave-length	starting point	2-year goal	Actually achieved
Defect Concentration	green blue	5E6 cm^{-2} 1E7	1E4 1E5	1E3 cm^{-2} 1E4
Threshold Voltage	green blue	9 V	4 V 7 V	3.3V 7.0 V
Doping of MgZnSSe	green blue	2E17 cm^{-3} 1E16		2E17 cm^{-3} 8E16 cm^{-3}
Device Process Dev.	green blue	index guided, epi-up	Opt.Rec. lasers index guided	Opt.Rec. lasers index guided
Recording Testing	green		read demo.	DVD read demo.
Lifetime cw, 2 mW	green blue	0.1 sec	50 hr 5 min	57 h 2 min
Lifetime 20 mW, 10%	green	0.1 sec	10 hr	6 h

Table I. Technical Goals

Judged by these technical goals, this program has been an overwhelming success. Almost all of the original goals have been demonstrated.

The remainder of this report describes these results in detail.

University Subcontracts

This contract supported three university subcontracts. All of these were seen as high-risk, long-range projects best suited for university research. The results of this work are briefly summarized here.

One subcontract (Columbia University, Professor Wen Wang) explored the use of arsenic as an alternative p-type dopant. The approach used a novel, extremely high temperature As cracking cell. The cell was designed, fabricated, tested and used to grow ZnSe:As. Although As was incorporated in the ZnSe, *p*-type conductivity was not achieved.

A second subcontract (University of Florida, Professor Robert Park) was used to develop homoepitaxial growth of ZnSe on ZnSe substrates. This was seen as a "fall-back" approach, in case problems surfaced with the use of GaAs substrates. The quality of available ZnSe substrates (from Sumitomo Electric Industries) was poor compared to

ZnSe heteroepitaxy on GaAs. However, significant advances were made in the preparation of the ZnSe surface for homoepitaxy.

The third subcontract (University of Florida, Professor Robert Park) involved the use of a novel plasma source for use with phosphorus as a p-type dopant. Preliminary results have demonstrated phosphorus is incorporated into ZnSe epitaxy . Some limited *p*-type conductivity has been achieved. Research continues in this area, although the preferred *p*-type dopant for II-VI compounds at this time is still clearly nitrogen.

II-VI Semiconductors

The II-VI semiconductors make up a remarkably rich palette of materials, covering band gaps from deep in the ultraviolet to semimetals (e.g., HgSe.). Figure 1 plots the band gap of most II-VI compounds versus their lattice parameter. Several important alloy systems are high-lighted.

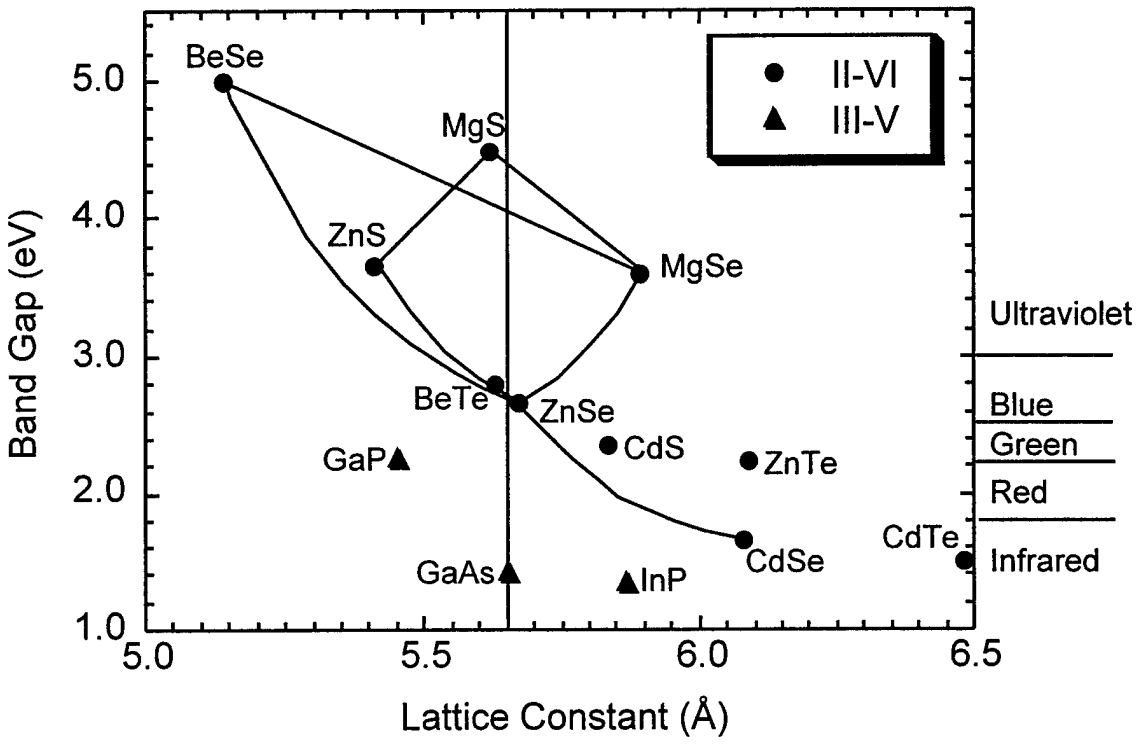

Figure 1. II-VI semiconductors and alloys

To fabricate II-VI blue-green lasers, the substrate of choice is GaAs. When compared to alternative ZnSe substrates, GaAs offers higher electrical and thermal conductivity, larger diameters, lower cost and much higher crystalline quality. The slight difference in thermal expansion coefficients between GaAs and ZnSe has a negligible effect given that II-VI growth temperatures are typically less than 300°C. At the beginning of this program, there was some question regarding difficulties with the chemistry of the GaAs-

ZnSe interface. These issues have now been resolved, and the critical GaAs-ZnSe interface is well controlled.

Two important II-VI alloy systems that can be grown lattice-matched to GaAs substrates are MgZnSSe-ZnSSe and BeMgZnSe-BeZnSe. Lasers based on either system are routinely grown with no misfit dislocations.

The CdZn(S)Se alloy system is used for the light-emitting quantum well. This alloy is not lattice matched to the GaAs, but is compressively strained. The quantum well is thin enough (< 50 Å) to be pseudomorphic--free of misfit dislocations.

2. *P*-type Doping

While nitrogen doping using a plasma source and molecular beam epitaxy has been the only successful method of fabricating II-VI laser diodes, it has provided a far from perfect *p*-type dopant. Achievable N_A-N_D levels strongly depend on the bandgap of the specific II-VI material. Maximum carrier concentrations of ZnTe:N can reach 10^{20} cm^{-3}, ZnSe:N is limited to $1x10^{18}$ cm^{-3} and MgZnSSe:N ranges from $2x10^{17}$ to $2x10^{16}$ cm^{-3} as the bandgap energy goes from 2.79 to 3.1eV respectively. A plot of N_A-N_D values for MgZnSSe:N can be seen in Figure 2. Values can vary slightly with flux ratio and growth temperature but the overall N_A-N_D behavior stays the same. The inability to effectively dope wide bandgap quaternaries (Eg > 3.0 eV) has been the limiting factor in II-VI diodes not being able to go to shorter wavelength devices, i.e. practical devices with <480 nm.

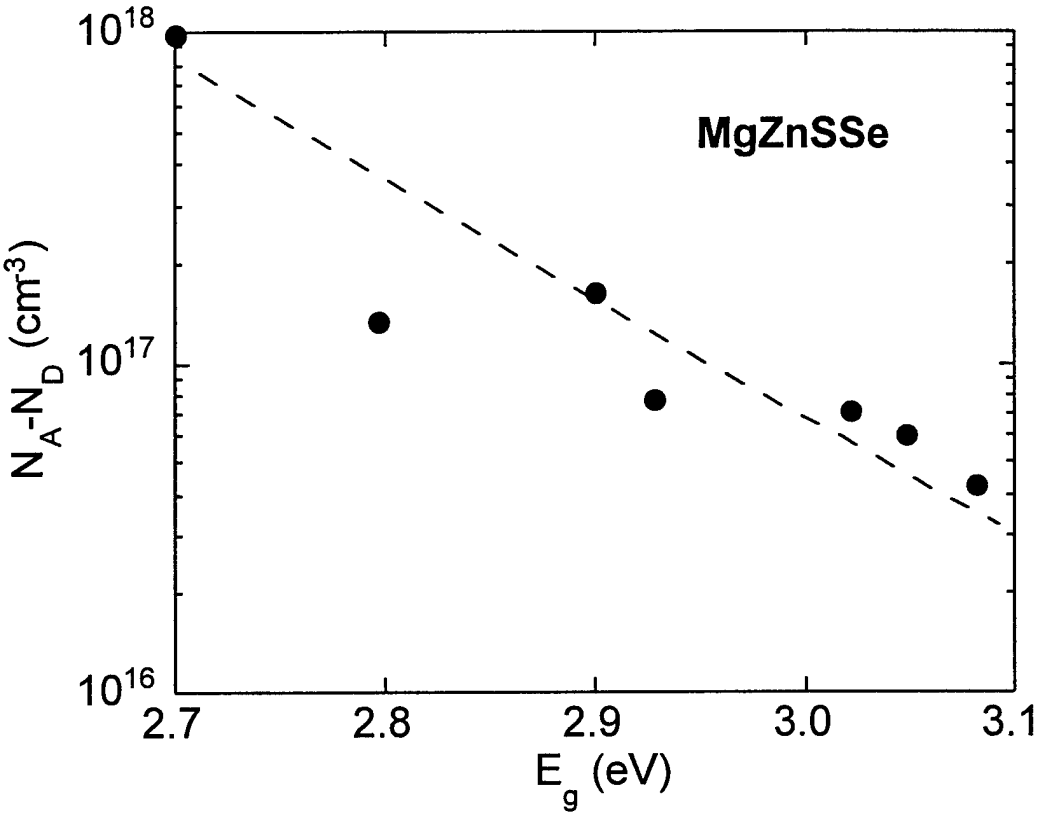

Figure 2. Graph of maximum achieved p-type doping as a function of band gap in MgZnSSe nominally lattice-matched to GaAs.

Total nitrogen incorporation, as measured by SIMS can be and usually is much higher than the N_A-N_D value. With increasing nitrogen incorporation the samples become compensated and N_A-N_D reduces to the point that the sample will be semi-insulating. In the case of ZnSe, grown with optimum conditions, nitrogen concentration as measured by SIMS and the N_A-N_D track one to one up to a value of approximately $3x10^{17}$ cm^{-3}. With increasing doping compensation eventually becomes severe, limiting N_A-N_D to less than $2x10^{18}$ cm^{-3}. The microscopic behavior of excess nitrogen, that is nitrogen that does not fall on a selenium site, is not clear. However, nitrogen, unlike lithium, does not seem to be susceptible to electromigration. We have also performed studies to determine the nitrogen diffusion coefficient of ZnSe:N, where the nitrogen concentration was such that the vast majority fell substitutionally at Se lattice sites. In that regime, an anneal at 300 °C for 72 hours showed no diffusion of the nitrogen within the measurement limits of SIMS.

3. Ohmic Contacts

Low resistivity ohmic contacts are important to the operation characteristics of laser diodes due to the high current densities required. In the case of II-VI laser diodes, low resistivity ohmic contacts to the n-type side of the diode were easily obtained for several reasons. First of all, ZnSe based materials are easily doped n-type with doping densities as high as 10^{20} cm^{-3} reported. Therefore, many metals can be used to make a good ohmic contact. The barrier created by the difference of the metal work-function and the conduction band of ZnSe can be made sufficiently thin by increasing the doping of the ZnSe layer. Secondly, ZnSe based devices are often grown on GaAs substrates, and since there is a minimal conduction band offset between GaAs and ZnSe, a minimal barrier to electron flow across this interface is found. Because of these two conditions, diodes can be made either n-type up or down and still achieve good contact to the n-type side of the device.

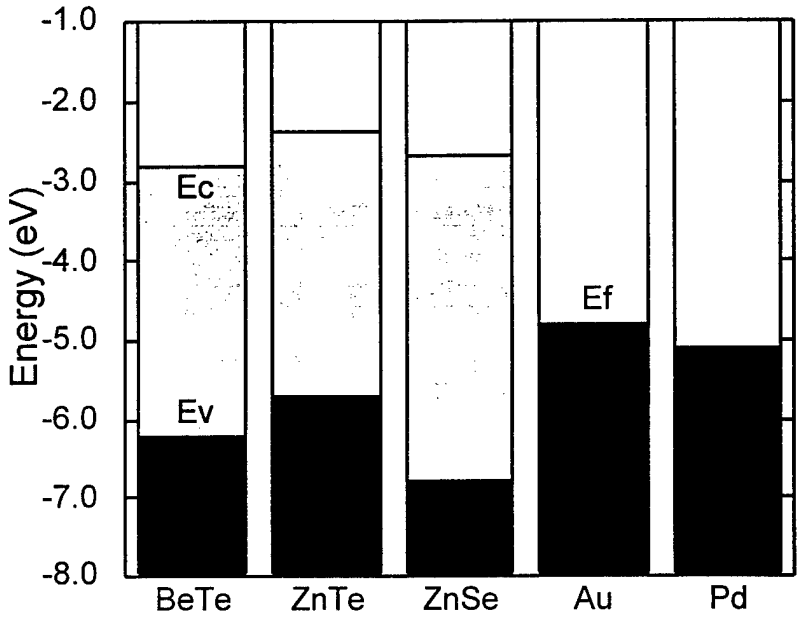

Figure 3. Relative energy levels with respect to the vacuum.

Unfortunately, contacting the p-type side of a ZnSe based diode is not as straightforward as contacting the n-type side of the device. Difficulties in contacting the p-type side of a ZnSe based diode arise from two sources. First of all, the valence band of ZnSe does not line-up well with any metals or the GaAs substrate as can be seen in Figure 3. Because of the energy difference between the work function of any contact metal and the ZnSe valence band, a barrier to the flow of holes is formed. In principle, this barrier could be made to be thin enough to provide a tunneling path through the barrier by heavily doping the ZnSe . However, ZnSe can only be doped p-type to about $1x10^{18}$ cm^{-3}. This rather low doping density does not reduce the barrier thickness enough to reduce the contact resistance of the devices. Therefore, another means of providing a low resistance p-type contact to ZnSe was needed. The first step in developing a useful contact came with the

demonstration of high *p*-type doping of ZnTe. Because ZnTe has a more favorable valence band energy position and can be heavily doped *p*-type a low resistance contact can be made easily to *p*-ZnTe. The problem then becomes the barrier to hole flow between *p*-ZnSe and *p*-ZnTe. The ideal method of overcoming this is through the use of a graded alloy of $ZnSe_xTe_{1-x}$ where x would vary from one to zero over the thickness of the contact structure. However, it is very difficult to reproducibly grow $ZnSe_xTe_{1-x}$ (described below).To achieve the desired structure without growing the alloy $ZnSe_xTe_{1-x}$, a pseudo-alloy was used. A pseudo-alloy consists of thin alternating layers of binary materials, in this case ZnSe and ZnTe. By varying the ratio between the thicknesses of the binary material the effective composition can be controlled. A schematic diagram of the structure is shown in Figure 4.

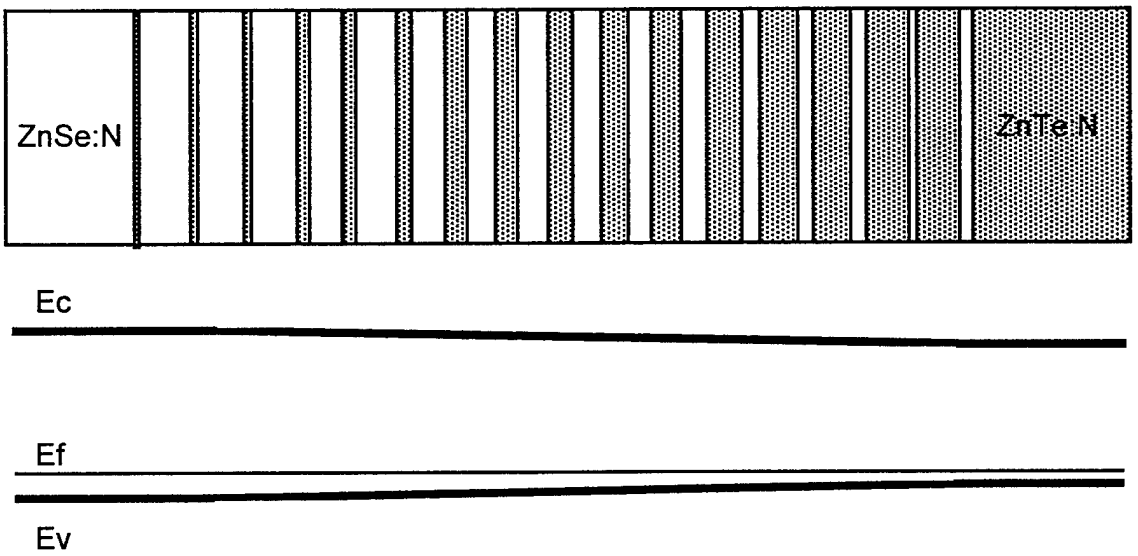

Figure 4. Digital grading of ZnSe-ZnTe:N ohmic contact. The ZnSe layer thickness decreases linearly from 17 Å to 2 Å, while the ZnTe layer thickness increases from 2 Å to 17 Å.

Although the ZnSe/ZnTe pseudo-graded contacts were a breakthrough in the area of ZnSe based laser diodes, they are not without significant problems. The reproducibility of the contact resistance and voltage is a problem. The transport characteristics of this structure are very sensitive to the MBE growth conditions; yet it is unclear which growth parameter is critical. It is clear that if the growth temperature is too high, compensating defects diffuse from the contact to the underlying layers. These diffusing defects then produce a highly resistive layer under the contact which dramatically increases the operating voltage of the device. Another shortcoming of the ZnSe/ZnTe pseudo-graded contact is the relatively short lifetime of the structure. The ultimate lifetime goal of the II-VI laser diodes is greater than 10,000 hours, however the transport characteristics of these structures degrade in as short at a couple of hours to as long as a few tens of hours. Although the cause of the transport degradation is unknown at this time, there is a possibility that the many crystalline defects that are found in the structure could play a

role in the degradation. These defects form as a consequence of the lattice mismatch between ZnTe and GaAs.

ZnSeTe alloys for contacts

To improve ZnTe based contact performance, we explored the use of a $ZnSe_{1-x}Te_x$ alloy as replacement for the ZnTe in the digitally graded layers. The motivation behind this concept stems from our work growing $ZnSe_{1-x}Te_x$:N compositions and measurement of the specific contact resistance using Au contacts (Figure 5). The use of a thin Pd then Au deposition and low temperature anneal can improve by nearly an order of magnitude the specific contact resistance achievable. From this plot one can see that $ZnSe_{1-x}Te_x$ with a x value of 0.33 still offers a respectable contact resistance. This same composition can have a N_A-N_D value of greater than 10^{19} cm^{-3} as measured by CV. The advantage of this scheme is that the valence band difference between $ZnSe_{1-x}Te_x$ and ZnSe would be less than that between ZnTe and ZnSe, hence making tunneling easier and the potential drop across the digitally graded layer less. Another possible advantage would be that there is less of a lattice constant difference in going more toward ZnSe compositions on GaAs substrates, offering a possibility of a pseudomorphic contact.

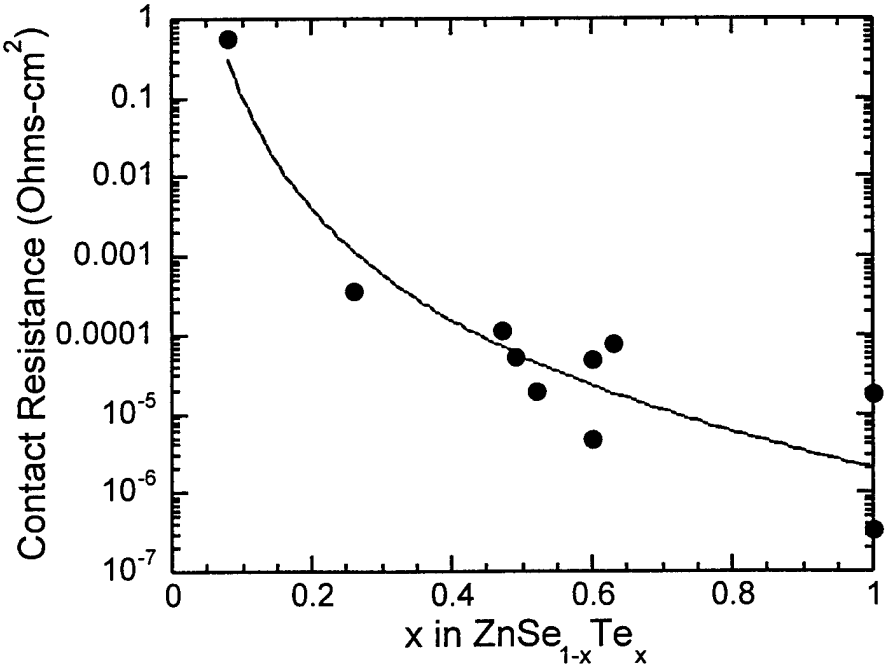

Figure 5. Dependence of measured contact resistance on ZnSeTe composition.

There was initial difficulty in growing the ternary compositions, as they tended to become amorphous within a few thousand angstroms of growth. It was found that the best ternary growth conditions were under metal rich conditions with a flux ratio of nearly 10:1 as measured by a thickness monitor. When composition and doping control were obtained for the ternary, $ZnSe_{0.33}Te_{0.67}$:N was applied to our existing contact

structure as a replacement for the ZnTe:N layers. The resulting contacts showed a large fully depleted ZnSe:N region well below the graded region. This observation was similar to, but greatly magnified from that we had observed when we had overdoped the ZnTe contact. Under conditions of overdoping we had seen what we believe to be a diffusion of a nitrogen-related point defect (interstitial N or selenium vacancy) at growth temperature into the previously grown layers during growth as supported by PL and electrical measurements. Other researchers have observed diffusion of nitrogen during growth of similar contact structures using SIMS and PL studies.[4] In the case of an overdoped ZnTe contact the depleted layer could be at most a kÅ but with $ZnSe_{0.33}Te_{0.67}$:N contact the depletion region could extend many kÅ as measured by CV at a variety of etch depths. PL of ZnSe:N below the graded region in both cases was consistent with highly compensated material. Our solution to the problem was to reduce the nitrogen doping in the ZnSeTe and varying the grading scheme. Unfortunately, by the time we were able to reduce the nitrogen doping to the point where we were no longer compensating the underlying ZnSe, we were left with a highly resistive graded region. In only one case did we have any success in this endeavor and that involved the growth of a single $ZnSe_{0.33}Te_{0.67}$:N (500Å) on ZnSe:N. This contact yielded a V(500 A/cm^2) of 7 volts, but the contact was very unstable and short lived.

TEM of ZnTe and BeTe contacts

The large lattice mismatch (~8%) between ZnSe and ZnTe gives rise to a high microstructural defect density in the contact region, as is shown in Figure 6. The defects may play a role in contact degradation. Nitrogen dopants in the contact region may be compensated by the high defect density. Since BeTe, with a bandgap of 2.8 eV, is closely lattice-matched to ZnSe, BeTe layers with ZnSe-BeTe:N digitally graded layers appear an ideal candidate for ohmic contact to *p*-ZnSe based semiconductors. BeTe can be grown pseudomorphically to a thickness of 500 - 1000 Å (compared to several Å for ZnTe). Indeed, the BeTe contacts exhibit high-quality layer structure with low defect density as is shown in Figure 7.

[4] A. Taike, M. Momose, K. Kawata, J. Gotoh, K. Mochizuki, and S. Nakatsuka, Appl. Phys. Lett. **68**, 388 (1996)

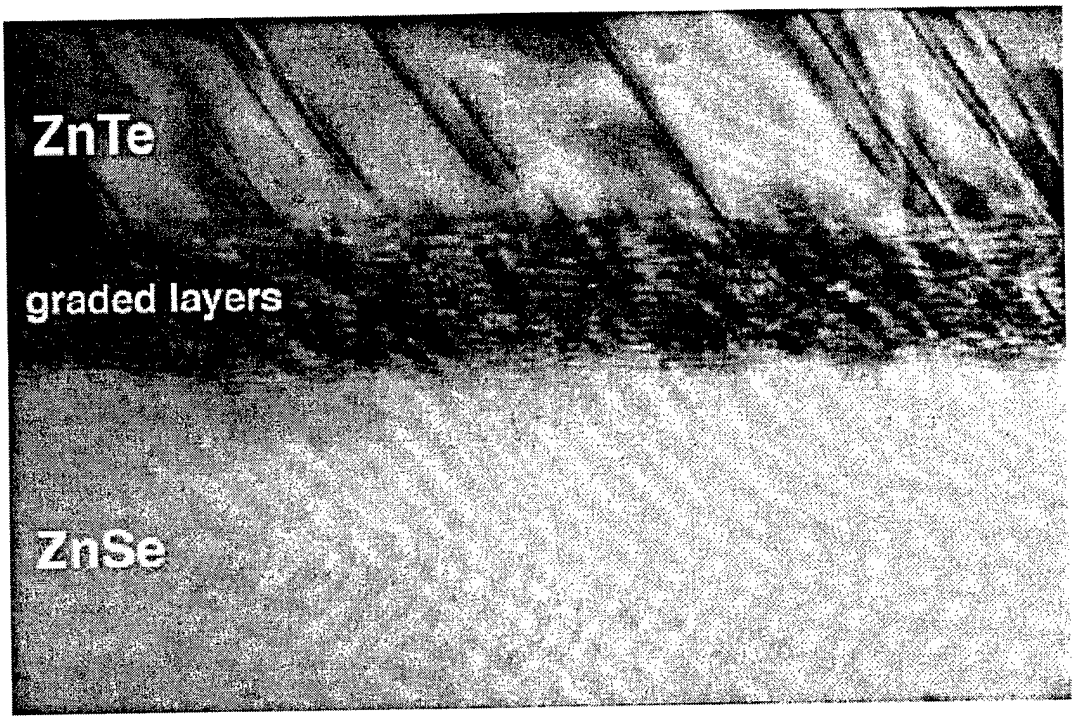

Figure 6. Cross-sectional TEM of p-ZnTe contact on p-ZnSe.

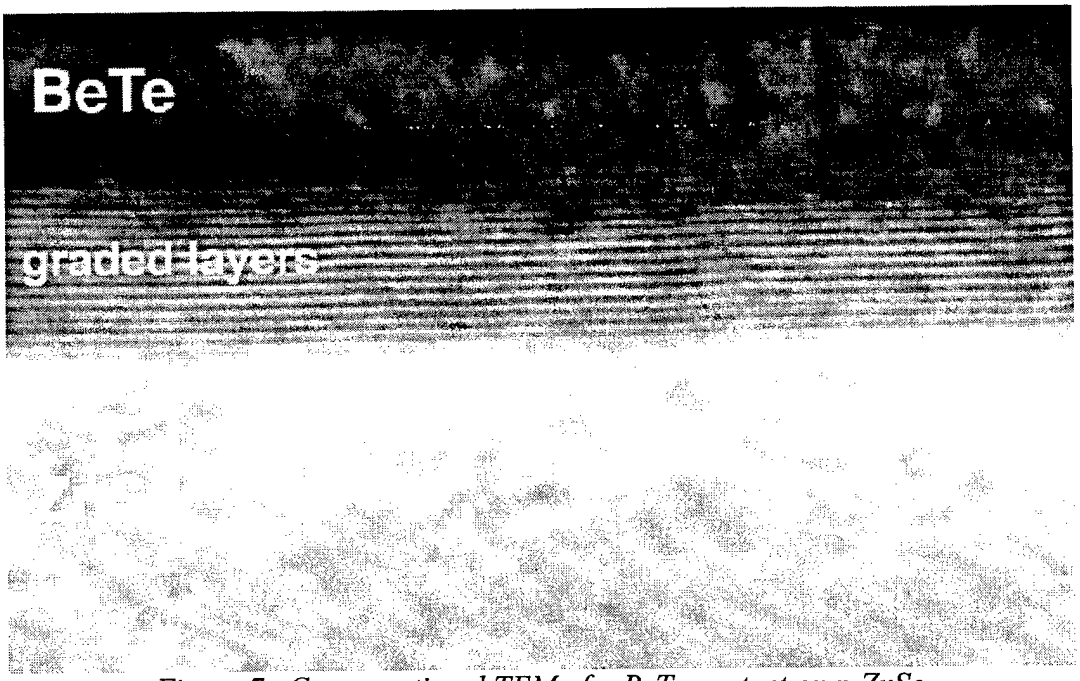

Figure 7. Cross-sectional TEM of p-BeTe contact on p-ZnSe.

We have grown many *p*-type ohmic contact structures and tested them for contact longevity. These structures generally consist of a ZnSe buffer on GaAs, a layer of *p*-type BeMgZnSe, followed by the p-type (ZnSe-BeTe) graded contact. At elevated test currents (2000 A/cm^2), we have demonstrated contact lifetimes of over 1600 hours, an improvement of 100 times over the conventional ZnTe contact (Figure 8).

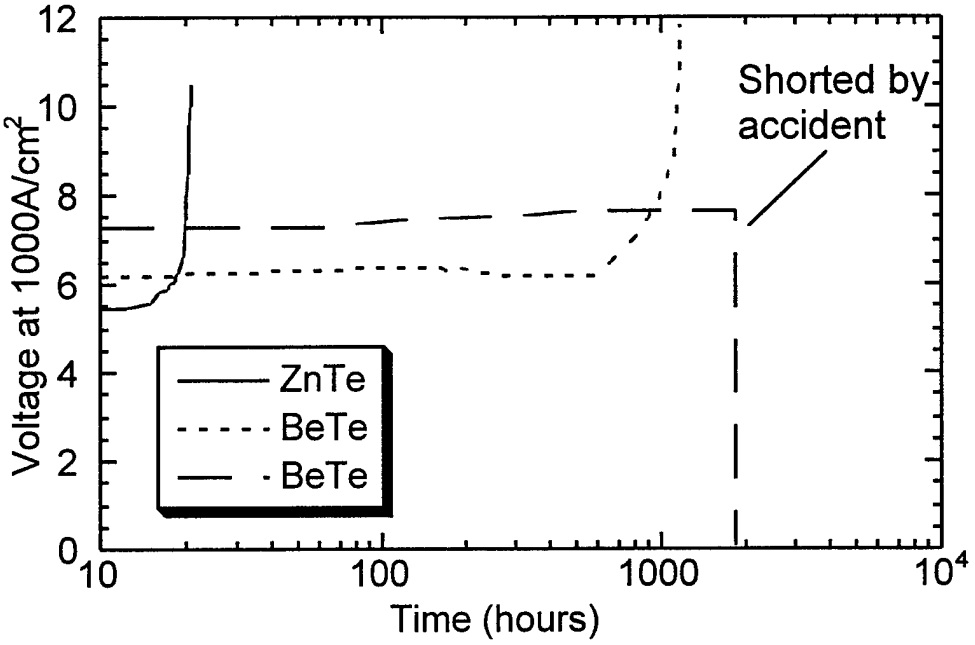

Figure 8. Lifetime performance of three p-type ohmic contact structures when operated at 1000 A/cm^2.

4. Be-based *vs* S-based Lasers

Before this work, blue-green II-VI separate confinement heterostructure (SCH) lasers were based on the S-containing compounds, MgZnSSe and ZnSSe. This "conventional" design is summarized in Table II. Laser diodes consisting of these S-based compounds can suffer from poor composition control, stacking fault defects, and short *p*-type ohmic contact lifetime. Each of these issues is addressed by the inclusion of Be into the laser structure.

S-based	Function	Thick (μm)	Eg (eV)	Be-based
ZnTe:N	ohmic	0.05		**Be**Te:N
ZnSe/**Zn**Te:	graded	0.03		ZnSe/**Be**Te:N
ZnSe:N		0.1		ZnSe:N
MgZn**S**Se:N	cladding	1.0	2.85	**Be**MgZnSe:N
Zn**S**Se	waveguide	0.15	2.7	**Be**ZnSe
Cd**Zn**SSe	quantum well	.0004	2.4	CdZnSe
Zn**S**Se	waveguide	0.15	2.7	**Be**ZnSe
MgZn**S**Se:Cl	cladding	1.0	2.85	**Be**MgZnSe:Cl
ZnSe:Cl	II-VI buffer	0.1		ZnSe:Cl
GaAs:Si	III-V buffer	0.2		GaAs:Si
n:GaAs	substrate	3000.0		n:GaAs

Table II. This laser material stack diagram shows the common S-based structure (left), the Be-based structure (right) and the layer description (center).

We have grown and fabricated Be-based II-VI SCH laser diodes consisting of ZnSe buffer layers, BeMgZnSe cladding layers, BeZnSe guide layers, and *p*-type contact layers digitally graded from ZnSe to BeTe[5]. This design is summaried in Table II. The room-temperature bandgap of the quaternary cladding layers typically range from 2.85 to 2.90 eV, while that of the lattice-matched ternary guide layer is 2.75 eV. Because Be has a much higher sticking coefficient than S, composition control is greatly enhanced. For example, the FWHM of a typical quaternary X-ray peak is ≥ 10 arcsec, the limit of the measurement technique. Day-to-day reproduciblity of composition is also improved, as the X-ray peak positions for the Be quaternary and ternary layers are easily maintained within approximately 150 arcsec of the substrate. Typically, gain-guided laser devices have threshold current densities of less than 500 A/cm^2 and voltages of 4 - 5 V (See Figure 9). The emission wavelength is approximately 515 nm.

[5] "Beryllium-Based II-VI Blue-Green Laser Diodes," T. J. Miller, P. F. Baude, G. M. Haugen, M. A. Haase, D. C. Grillo, F. R. Chien and M. D. Pashley, LEOS 1996 Conference, November 18-21, 1996, Boston, MA.

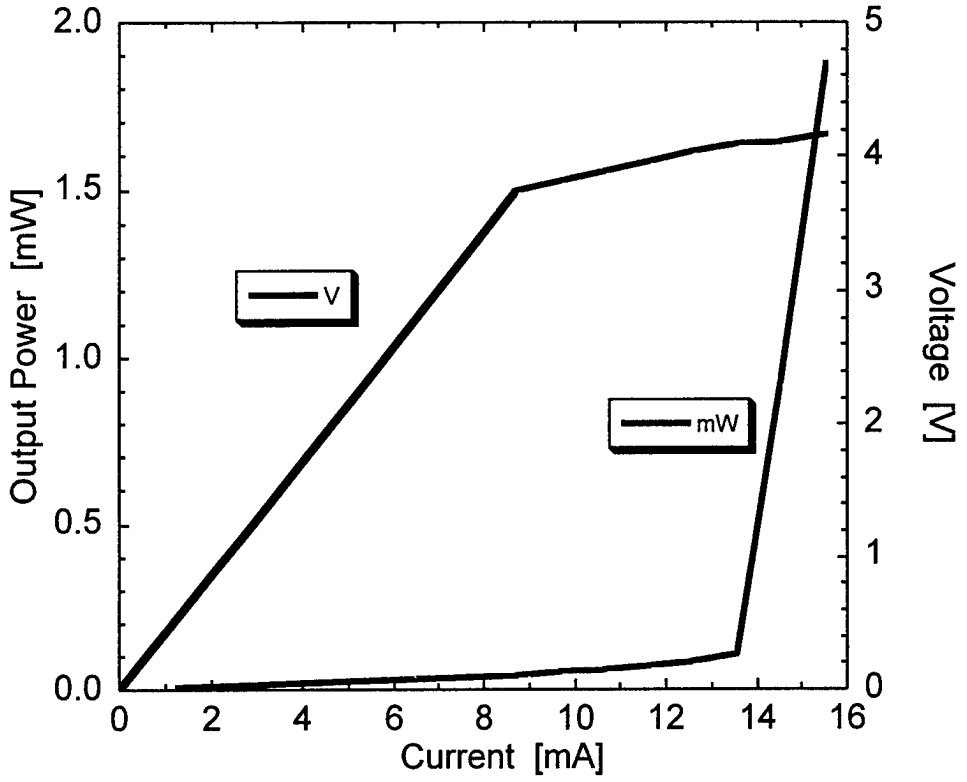

Figure 9. This is a typical L-I-V curve of a facet-coated buried ridge device fabricated from the same material that exhibited our record 57 hours lifetime. The operating voltage is roughly 4 V, and the threshold current is 13.5 mA (350 A/cm^2).

Since our report of the first Be-containing laser (which had a lifetime of 65 min.), we have grown and fabricated another such laser which operated for 57 hours (See Reliability Section). The defect density in this sample (which was grown before our more recent, lower-defect density ZnSe growth initiation procedure) was determined by various techniques to be 9000/cm^2.

In the *p*-type ohmic contact, the ZnTe is replaced by BeTe which has a critical thickness of approximately 1000 Å (compared to several Å for ZnTe). The resulting Be-containing contact layers are essentially free of stacking faults, whereas the ZnTe contacts generally have over 10^6/cm^2 (See Ohmic Contacts Section).

5. Laser Fabrication and Testing

Two types of laser diodes have been fabricated using II-VI epitaxial materials; gain-guided and index-guided devices. The gain-guided devices are more easily and reproducibly fabricated and are the preferred design for rapid and reliable feedback on the quality of the epitaxial materials. The are used to characterize lasing wavelength, and threshold current density and voltage (Figure 10). However, index-guided lasers are required for many applications—particularly for optical data storage.

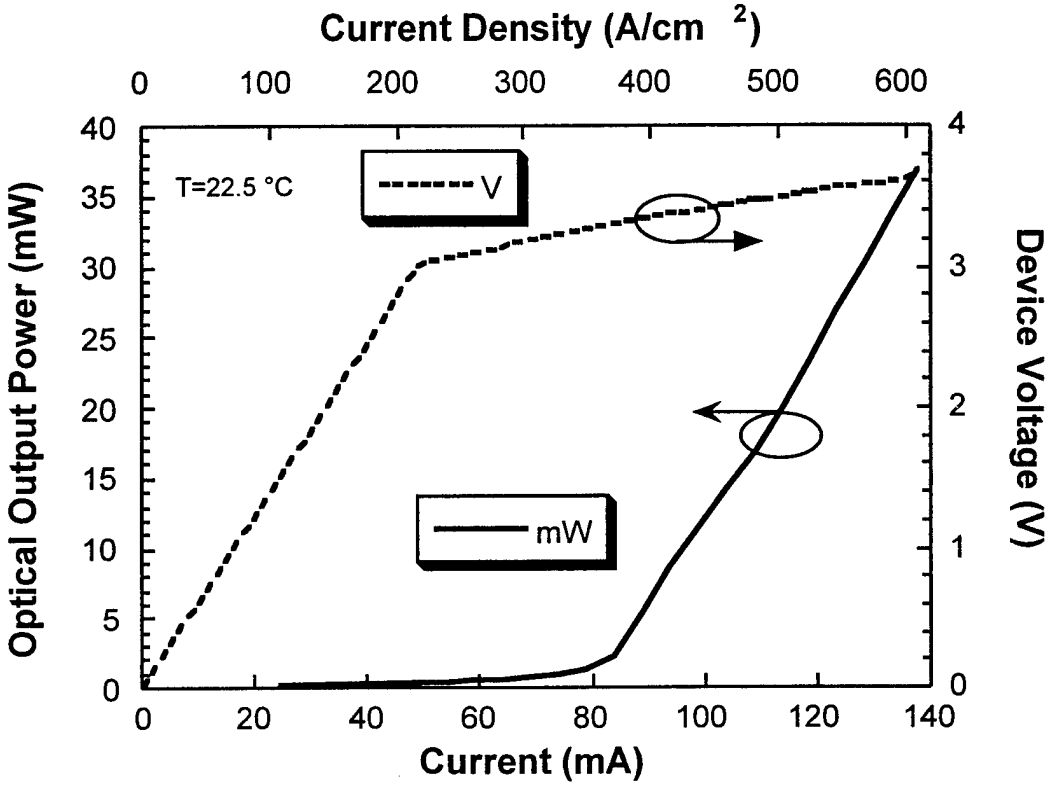

Figure 10. Characterization of a simple gain-guided II-VI device operating CW at 515 nm at room temperature. The CW threshold current density is about 356 A/cm^2 with a slope efficiency of about 30%. This device did not have facet coatings. The device voltage at threshold is 3.3 volts

Specifications for Optical Data Storage

As a guide for design of II-VI blue-green laser diodes, one may look to the existing specifications for red laser diodes for optical data storage applications. These requirements are summarizes in Tables III and IV. Also listed in these tables are the comparable measured performance characteristics of the 3M blue-green laser diodes. The excellent performance of the II-VI laser diodes is in part due to design and fabrication of index-guided structures based on 3M proprietary buried-ridge process technology. This process is described in the next section.

Parameter	Test Conditions†			Limits		Data	
Parameter Name	Symbol	Opt. Pow. (mw)	Temp (°C)	Min.	Max.	3M	Units
Astigmatism		1	25		+10	7	μm
Transverse mode		1, 30	25		1	1	mode
Polarization ratio		1	25	20:1		50:1	
Threshold Output	P_{th}		25		0.60	0.25	mW
Pulse Power			25	55		>100	mW
Pulsed Voltage		55	25		2.8		V
Characteristic Temperature	T_0		25-60	100		150	K
Wavelength	λ	30	25	676	695	515	nm
Far Field - FWHM Parallel to junction	$\theta_{\parallel}$	1	25	6	9	6	degrees
Far field - FWHM Perpendicular	$\theta_{\perp}$	1	25	16	21	24	degrees
Far Field Aspect ratio		1	25	2.0	2.6	4	

†Test conditions for 670 nm laser diode. In some cases the numbers for the blue-green laser diode were not measured at the same condition.

Table III. A comparison between 670 nm MO system laser diode specifications and current 3M 515 nm laser diode performance.

Parameter	Test Conditions†			Limits		Data	
Name	Symbol	Opt. Pow. (mw)	Temp (°C)	Spec. Min.	Spec. Max.	3M	Units
Power Output - CW			25	30		42	mW
Threshold Current	I_{th}		25	30	60	20	mA
Operating Current	I_{op}	30	25		110	40	mA
Operating Voltage	V_{op}	30	25		2.8	4-5	V
Differential Efficiency	η		25	0.6	1.0	0.75	mW/mA
Pulse Power			60	55			mW
Wavelength	λ	30	25	676	695	485-550	nm
Resistance	R	30	25	5	10	50	Ω
Capacitance	C	30	25	30	60	30	pF
Relative Intensity Noise	RIN	30	25	-125		-122	dB/Hz

†Test conditions for 670 nm laser diode. In some cases the numbers for the blue-green laser diode were not measured at the same condition.

Table IV. A comparison between 670 nm MO system laser diode specifications and current 3M 515 nm laser diode performance.

Fabrication Process Flow

Device processing of gain-guided lasers begins immediately after the substrate is removed from the growth chamber. The p-type semiconductor ohmic contact is briefly cleaned in a solution of HCl:H_20 (1:1) followed by a H_20 rinse and subsequently dried in N_2. The sample is moved directly into a vacuum chamber for deposition of the top metal contact. The p-type metal contact consists of Pd/Au, 50 Å and 500 Å thick respectively. A thin layer of titanium, 10 Å, is deposited on the Au to promote the adhesion of photoresist used in the next step.

The laser stripe is defined photolithographically using 5000 Å of negative photoresist and a photomask comprised of 20 μm lines on 500 μm centers. After the lines are delineated with photoresist the sample is introduced into a Xe^+ ion-milling system. The ion-mill acts to remove the metal-semiconductor ohmic contact outside the stripe. Polycrystalline ZnS is then thermally deposited with a thickness equal to that of the etched contact.

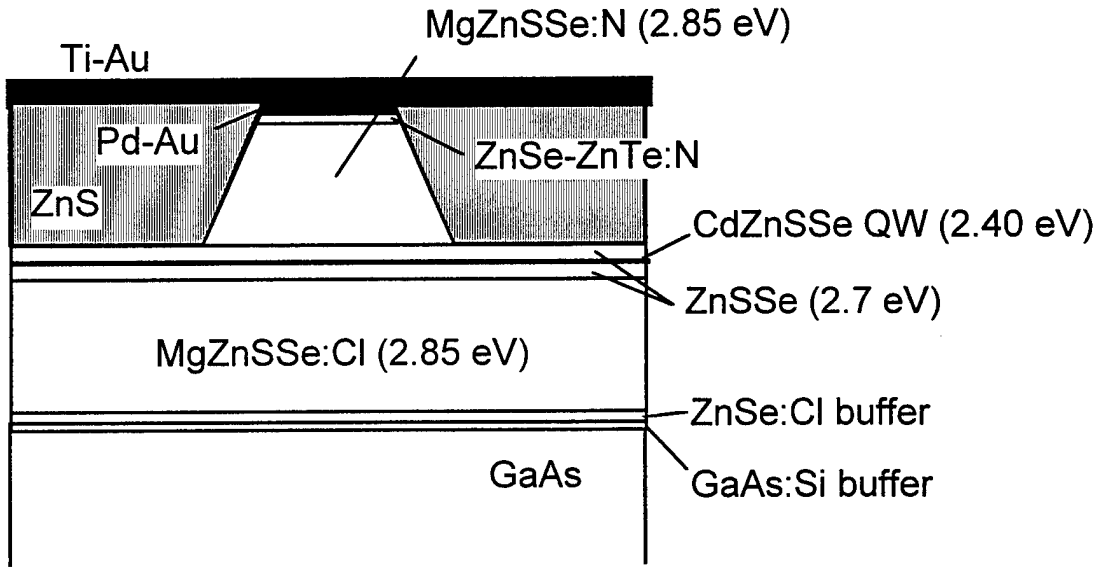

Figure 11. Cross-section of a MgZnSSe-based buried-ridge laser diode.

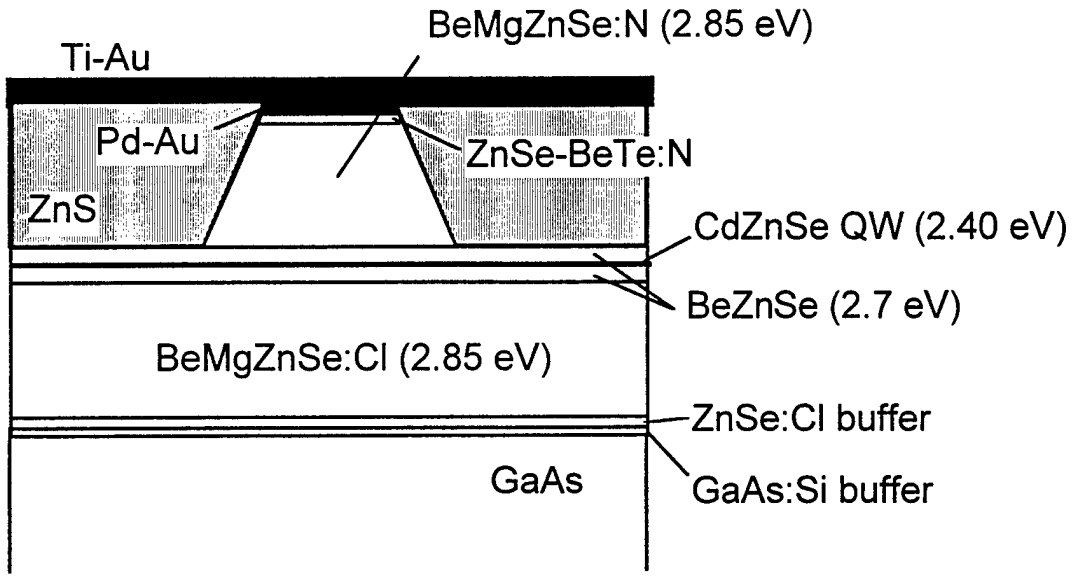

Figure 12. Cross-section of a BeMgZnSe-based buried-ridge laser diode.

Buried-ridge laser diodes are fabricated in a process quite similar to that described above for the gain-guided lasers (Figures 11 and 12). Departure from the gain-guided process, in fact, begins with the photolithography. Narrow lines, typically 4-5 μm wide, of photoresist are defined on the surface of the metallized semiconductor. The metal-semiconductor contact and underlying p-quaternary cladding layer are subsequently etched in the ion-mill. The depth of the etch is measured *in-situ* via a HeNe laser (λ=6328 Å) based interferometer. Interference of reflections between the sample surface and substrate / epi-layer interface is monitored using a simple silicon photodetector. This monitoring provides for precise control of the etch depth. Typically the cladding layer is ion-milled to within 2500 - 5000 Å of the guide layer. The ion-beam potential is reduced towards the completion of the milling process to minimize damage induced by Xe^+ ions driven into the crystal.

Zinc sulfide, is thermally evaporated onto the sample surface covering areas removed during the etching step as well as the photoresist used to define the ridge. The thickness of the polycrystalline ZnS is made equal to the ridge height, helping planarize the device. Cross-section optical and transmission electron microscopy of the ZnS layer reveals a c-axis oriented polycrystalline (Figure 13). Liftoff of the photoresist, and overlaying ZnS, completes the ridge definition and index-guiding layer deposition step. The process is identical for both MgZnSSe-based and BeMgZnSe-based laser diodes.

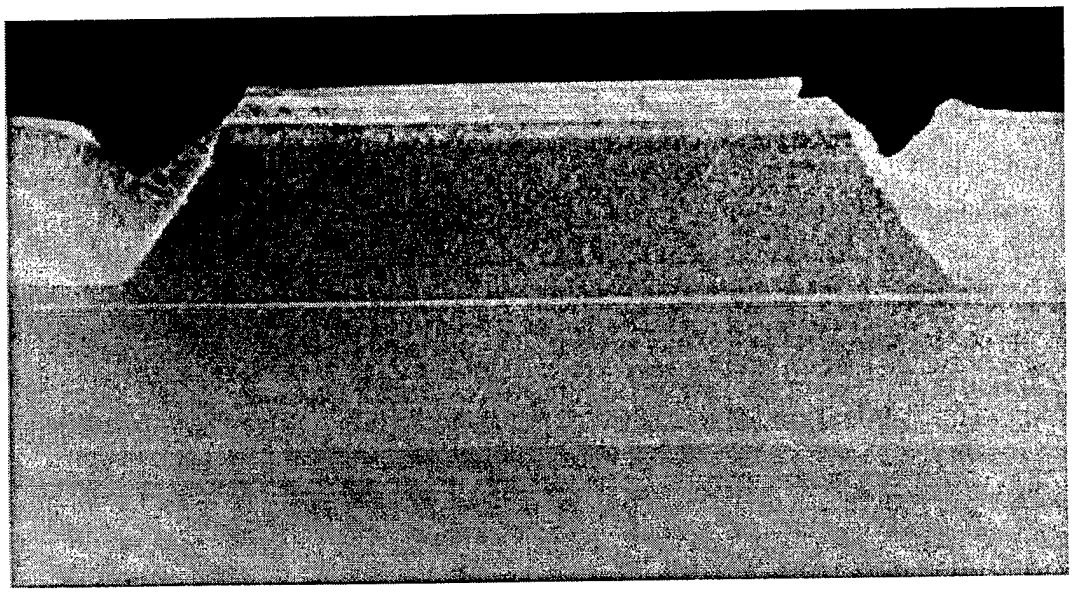

Figure 13. Transmission electron micrograph of cross-section of a 5-μm wide buried ridge laser diode. Polycrystalline ZnS burying layer nearly planarizes the etched surface and effectively covers the sides of the etched ridge. The bright line that crosses the middle of the image is the quantum well.

Both gain-guided and buried-ridge processing is completed by depositing a final "bond-pad" metallization of 500Å Ti - 2000 Å Au. Typically these bond pad are patterned into 200 μm wide stripes centered on the narrower active stripe of the laser.

The sample is then cleaved into bars typically 1 mm long. The bars are coated with quarter-wave dielectric reflectors to improve device operating characteristics. Thermally evaporated MgF_2 and ZnS comprise the alternating high and low index dielectric layers respectively. Typically, a high reflectivity mirror (R_f>90%) is deposited on the rear facet, while the front facet reflection coefficient is optimized for the desired optical output power.

The buried ridge device design provides much lower threshold currents (Figure 14) as well as excellent optical beam quality (Figure 15). Astigmatism is typically less than 10 μm.

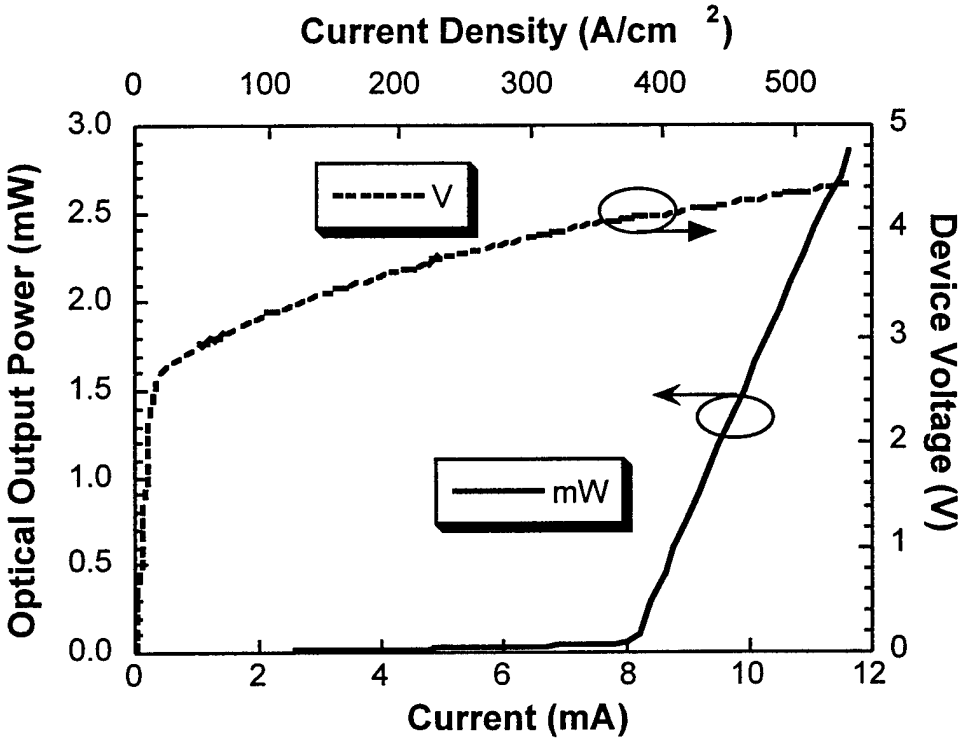

Figure 14. Characterization of an index-guided laser operating at 515 nm. The threshold current is 8 mA or 371 A/cm^2 for the 4 micron wide device. The slope efficiency is about 30%. This device was facet coated on the front and back facets; 70% and 95% respectively.

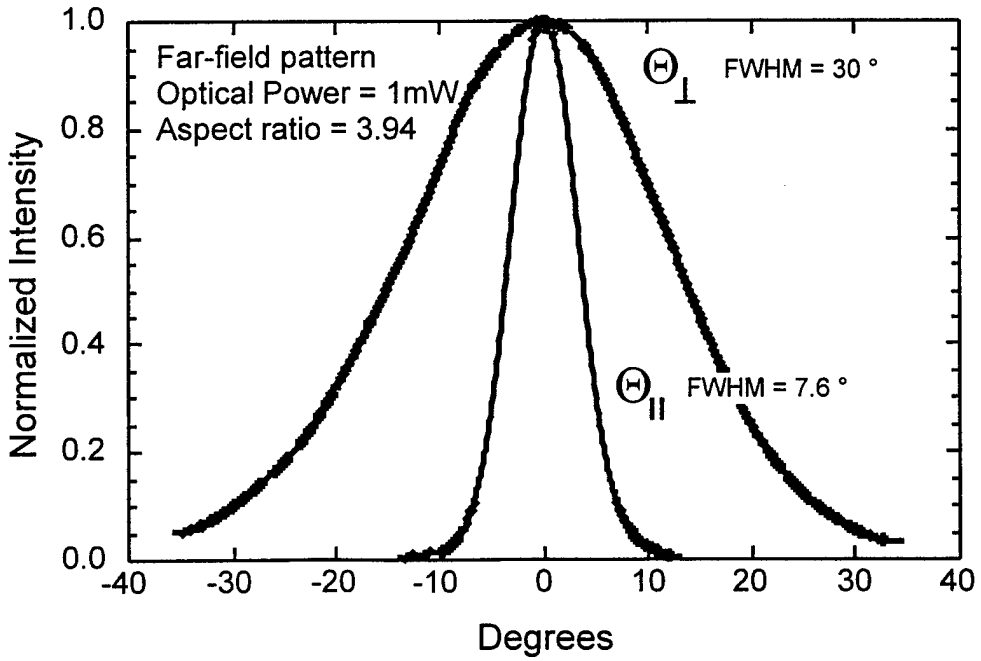

Figure 15. Room temperature far-field pattern of index-guided device operating at 1 mW per facet. The ratio of the perpendicular and parallel divergence, aspect ratio, is 3.94.

6. Reliability

Dark Line Defect Propagation.

The dominant failure mechanism in II-VI laser diodes is the growth of "dark-line defects" (DLDs). This mechanism is essentially identical that seen in the early development of AlGaAs laser diodes. During laser operation, the dark line defects grow from pre-existing crystallographic defects. In the case of AlGaAs lasers, these defects were dislocations that originated in the GaAs substrates. Over the years, GaAs substrates have become much better, and the dislocation density is now typically less that 10^{-3} cm^{-2}. In the case of II-VI laser diodes, the DLDs originate from stacking faults in the as-grown epitaxial layers. Our approach to improving II-VI laser reliability has been to eliminate these pre-existing defects.

Figure 16 illustrates the process of dark line defect propagation. This series of photographs are taken through a microscope looking down on a 20 μm wide gain-guided laser stripe. The laser is operated at 500 A/cm^2 which is just above threshold. The total time represented by this series of photos is about 30 min.

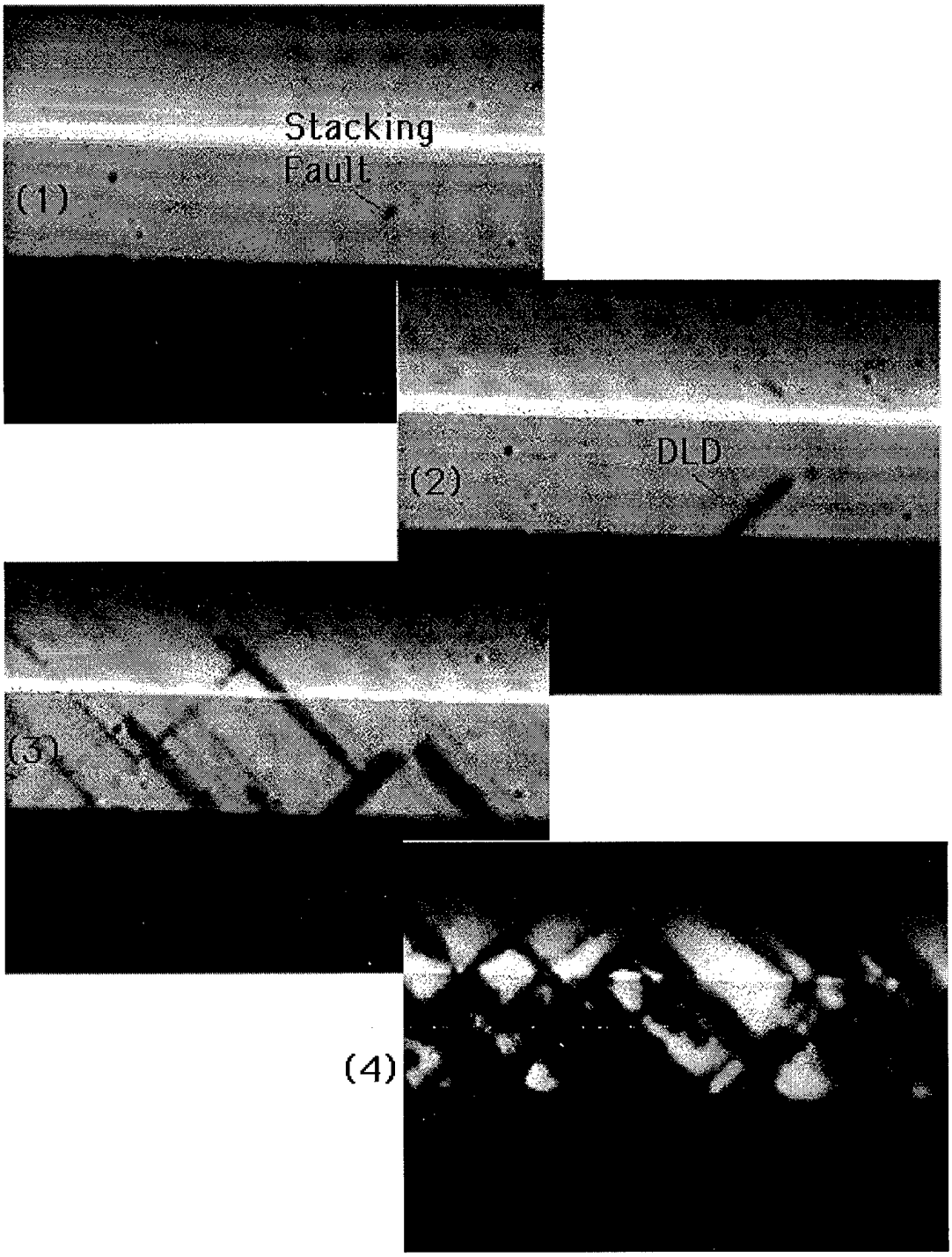

Figure 16. Series of electroluminescence photomicrographs showing laser failure by dark line defects.

Initially, a single stacking fault is revealed in the electroluminescence. Over time, as the device is operated, that stacking fault elongates and forms a dark line defect. These dark lines typically follow a <100> crystallographic direction. In addition, small mobile defects can sometimes be seen quickly moving along the same paths that the DLDs

follow. These mobile defects are very difficult to see in photographs. After further operation, the DLDs bifurcate and grow to eventually disable the laser operation.

Both the DLDs and the mobile defects are thought to be small dislocation loops and/or point defect clusters located in the quantum well. The growth and motion of these defects is driven by dark recombination. Initially, the dislocation associated with a stacking fault acts as dark recombination center. The energy released by this dark recombination at the extended defect is sufficient to cause the formation of a point defect (such as a Zn vacancy-interstitial pair). These point defects can coalesce into dislocation loops that themselves act as dark recombination centers and the process accelerates.

TEM of DLDs

A degraded laser device was characterized by cross-sectional TEM (Figure 17). The CdZnSe quantum well is typically 35Å thick and the interfaces are abrupt and initially free of microstructural defects. In order to observe the plane feature of a degraded quantum well, the cross-sectional TEM specimen was tilted ~30_ such that the plane of the QW was inclined to the electron beam. Typical DLDs are often arrow-shaped and they are only found within the quantum well. We suspect that DLDs result from the aggregation of dislocation loops, which are clusters of point defects.

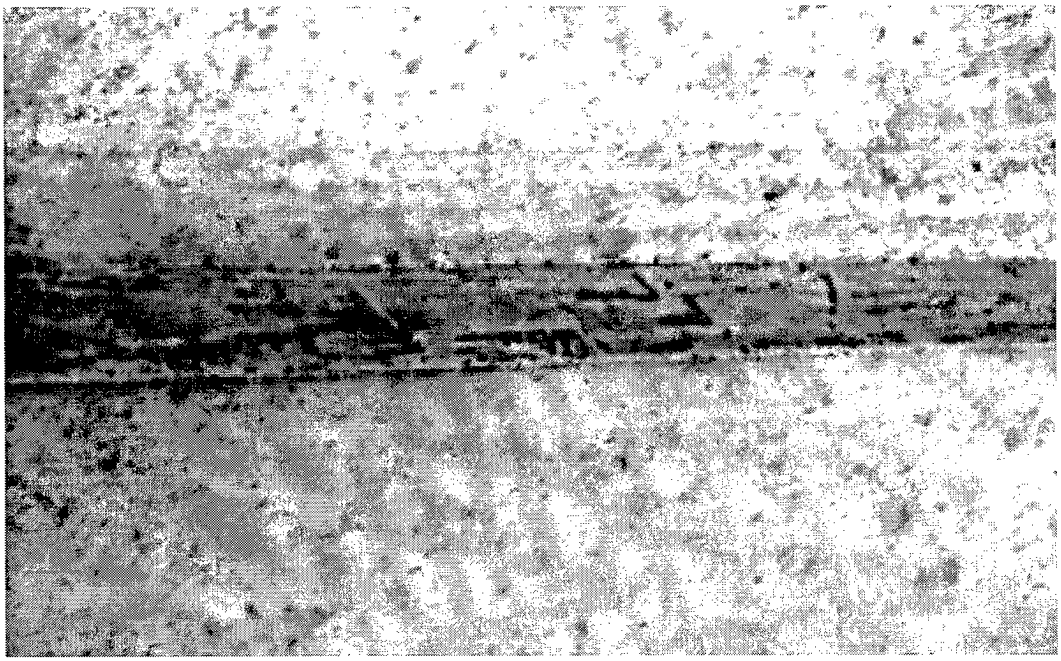

Figure 17. DLDs observed within a degraded QW in a TEM cross-sectional view.

TEM of stacking faults:

The dominant defect in as-grown II-VI lasers are bow-tie defects, which are pairs of triangular stacking faults. The typical bow-tie defects as revealed by TEM plan-view are shown in Figure 18. The paired defects are almost exactly the same size indicating that they nucleated at a common plane. The origin of these bow-tie defects was confirmed using cross-sectional TEM. When the planes of the paired stacking faults viewed edge-on, the paired-defects appear as a V-shape configuration as shown in Figure 19. These images confirm that bow-tie defects originate at the interface between the GaAs buffer and ZnSe buffer layers.

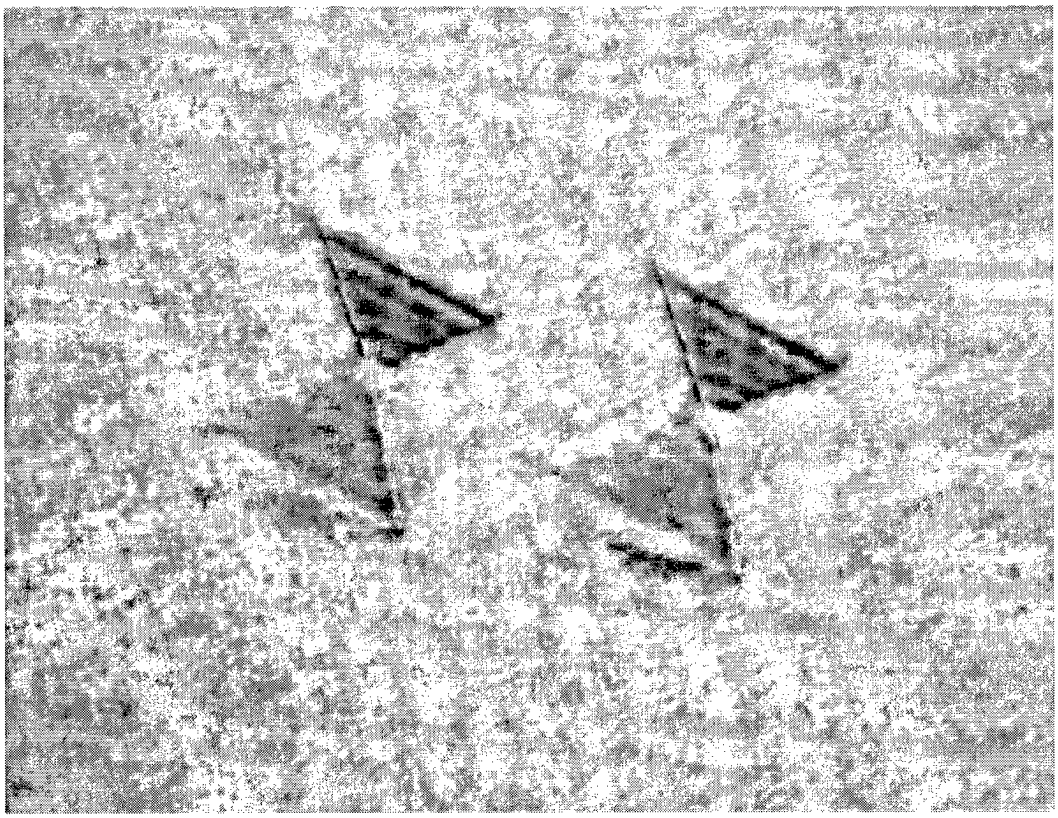

Figure 18. Typical bow-tie defects revealed by TEM plan-view.

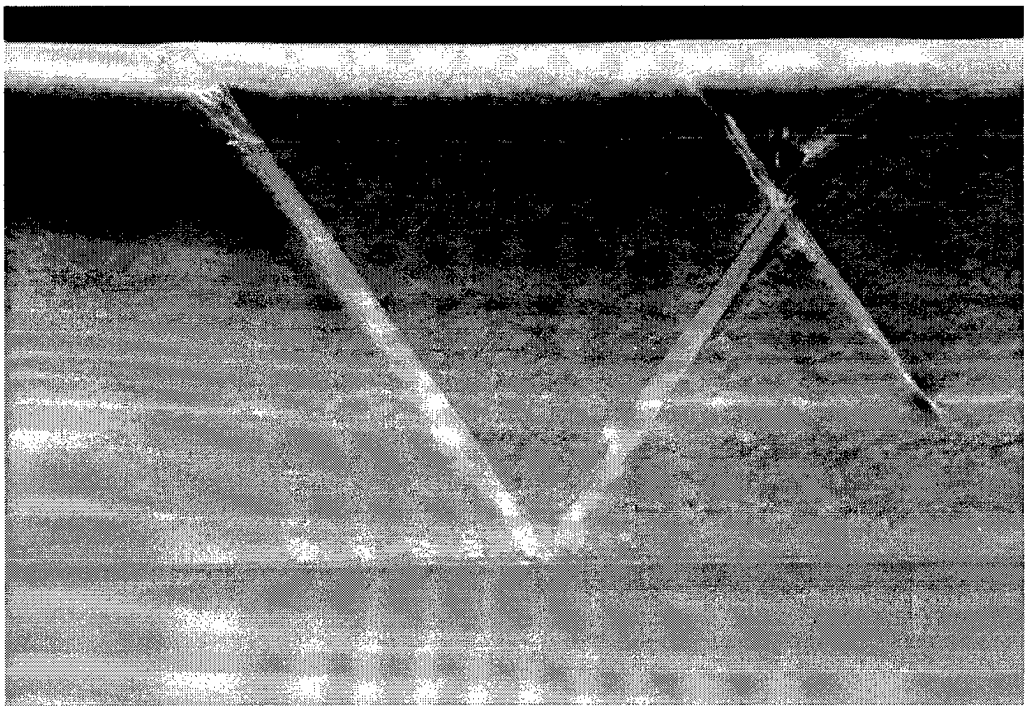

Figure 19. Bow-tie defects originated at the GaAs/ZnSe interface revealed by TEM cross-sectional view.

The origination of stacking faults

In general, the origin of a stacking fault (SF) is an inhomogeneity on or near the growth surface which interrupts the normal stacking sequence of atoms during growth. In our work, SFs usually occur at the interface between the GaAs and the ZnSe. In this case, an inhomogeneity could be in the form of 1.) an impurity atom or molecule on the surface, including background impurities in the vacuum chamber, or residual native oxide in the case of growth without GaAs buffer layers, 2.) a molecule resulting from a chemical reaction of the III-V/II-VI species at the interface, such as Ga_2Se_3 or Ga_2S_3, which have been shown to occur, or 3.) simply the imperfect growth of the ZnSe itself.

ZnSe defect reduction— growth procedures

We have concentrated our defect reduction efforts in an MBE chamber equipped to grow both GaAs and ZnSe (Interface Chamber). This chamber is equipped with standard effusion cells for Ga and Zn, and valved cells for As and Se. Since Se is known to be detrimental to the GaAs surface, the use of a valved cell here is of utmost importance. Likewise, a valved As cell is required, since excess As can result in the formation of ZnAs during the initial stages of ZnSe growth which may also result in a SF. By growing both the GaAs and ZnSe in the same chamber, the GaAs surface is not exposed to any more impurities than necessary, for instance in a transfer tube. Nor does the sample cool like it would during such a transfer, and therefore is less likely to condense an impurity.

Our growth sequence starts with the growth of a buffer layer of GaAs on the GaAs substrate at 600 °C. This serves to "bury" any residual native oxide or other surface contaminant which could originate a SF in the ZnSe. (Because the energy required to create a SF in GaAs is much higher than in ZnSe, this "burying" of a SF source in the GaAs is possible.) Another effect is to reduce the density of atomic step edges which are prevalent after desorbing the native oxide of the GaAs. Step edges expose Ga atoms slightly, and may thus be a sight for reaction with Se or S.

After the growth of the GaAs, the substrate is cooled in preparation for the growth of the ZnSe. During this cool-down, the As valve is closed at an appropriate time (as discussed below) to achieve a (2x4) As-terminated surface. When the substrate temperature reaches approximately 300 °C, the ZnSe growth is initiated by first exposing the GaAs surface to a flux of Zn. During this Zn exposure, the surface reconstruction changes from (2x4) to (1x4). This Zn treatment serves the purpose of separating the Ga from the Se, which can lead to the formation of Ga_2Se_3 as mentioned above. After the Zn treatment, the growth of about 100 Å of ZnSe commences by migration-enhanced epitaxy (MEE) (also known as atomic layer epitaxy or ALE). Finally, the ZnSe layer is grown to a thickness of approximately 500 Å by conventional MBE. This buffer layer is then ready to transfer to another chamber for the growth of a laser or other II-VI structure.

Correlation between surface prep (As-coverage) and EPD

As mentioned previously, exposed Ga on the surface of GaAs can react with Se to form a SF. Also, excess As can react with Zn and then form a SF. Thus, the SF density is a function of the surface preparation of the GaAs. We have found, congruent with the above simple arguments, that the As-terminated (2x4) GaAs surface gives the lowest SF density compared to the Ga-terminated (3x1) surface or the As-rich c(4x4) surface. However, a surface which nominally exhibits a (2x4) RHEED pattern may contain a homogenous (3x1) or c(4x4) surface reconstruction component, and thus result in a high SF density. To study this possibility, and to produce a process which reproducibly yields a perfect (2x4) surface, we performed the following experiment:

We grew several GaAs/ZnSe samples in succession as outlined above, and varied only the substrate temperature at which the As valve was closed during the cool-down following GaAs growth. When the As valve was closed at a substrate temperature below 520 °C, a c(4x4) surface persisted. When it was closed above 570 °C, a (3x1) surface persisted. For the samples within this range, the surface would first change to (3x1) (Ga-terminated), and then upon further cooling (but while still above approximately 420 °C) the (2x4) surface would reappear. We concluded that for substrate temperatures between approximately 420 °C and 520 °C, there is enough energy available for As atoms to travel from the bulk GaAs to the surface, but not enough to cause appreciable desorption off of the surface, which explains the reappearance of the (2x4) pattern in the absence of any external source of As. We speculated, then, that this process is a self-limiting method of achieving a (2x4) As-terminated GaAs surface. As shown in Table V (samples 1 - 6), the

samples for which the As valve is closed at a substrate temperature in the middle of the range from 520 to 570 °C yielded the lowest SF densities. If the As valve is closed too close to 520 °C, some amount of excess As may build up, while closing the As too close to 570 °C seems to result in an unrecoverable loss of As from the surface.

Samples 7 and 8 in the same table show the effect of the Zn treatment. Sample 7 was not exposed to a Zn flux prior to ZnSe growth, resulting in a high SF density. And though sample 8 was exposed to a Zn flux prior to ZnSe growth, the substrate temperature was too high for the Zn to stick, as witnessed by the persistence of the (2x4) RHEED pattern. The result is a high SF density.

Sample#	Substrate Temp. for Nucleation (°C)	RHEED Pattern prior to Nucleation	Substrate Temp. As valve closed (°C)	Zn Treatment	Stacking Fault Density (/cm^2)
1	315	(1x4)	520	yes	$1x10^4$
2	315	(1x4)	530	yes	$<1x10^4$
3	315	(1x4)	540	yes	$<1x10^3$
4	315	(1x4)	550	yes	$<1x10^3$
5	315	(1x4)	560	yes	$<1x10^3$
6	315	(1x4)	570	yes	$8x10^3$
7	315	(2x4)	550	no	$4x10^5$
8	330	(2x4)	550	yes	$6x10^6$

Table V. Various growth conditions and resultant defect densities.

Recent Lifetime Results

By transferring growth initiation methods that were formulated in the Interface Chamber, we have been able to achieve low-defect II-VI layers in the other two laser chambers. For single layers of ZnSe on GaAs, the SF density is generally less than 500/cm^2, which is the specified etch pit density of the GaAs substrates. We are able to grow full laser structures having defect densities less than 5000/cm^2 with a considerable level of reproducibility. This has led to dramatic improvements in device lifetimes. Or current "hero" device operated cw at room temperature for 57 h at 1 mW of output power (Figure 20).

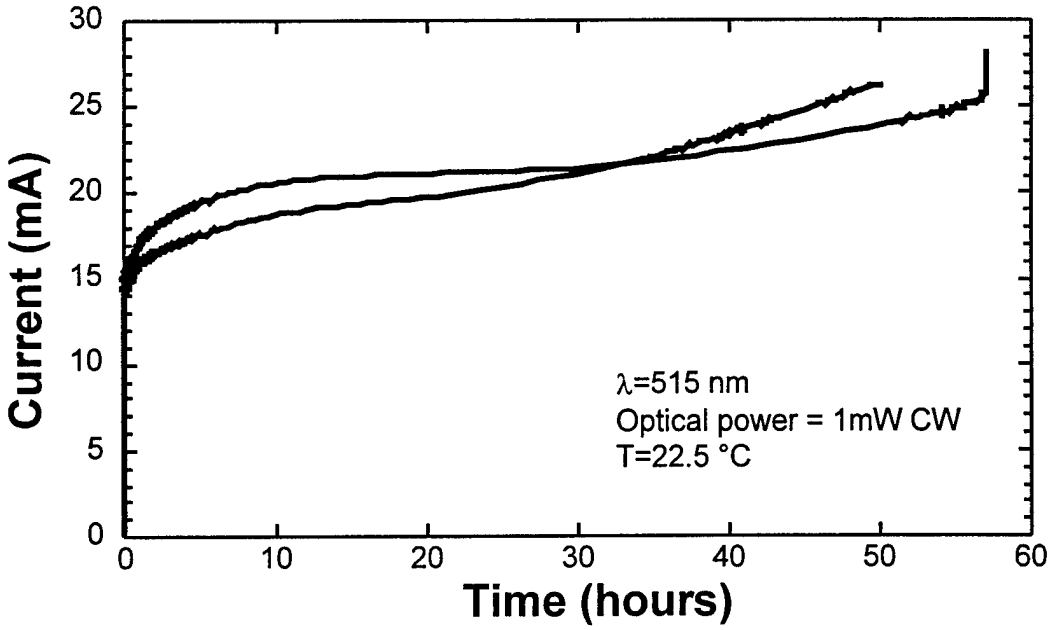

Figure 20. Measured current of two facet-coated index-guided lasers operating at 1 mW optical power. The lifetime of the device was defined as the time taken for the required current to double from the initial value. The two devices represent the longest lived lasers measured in our laboratory, 57 hours and 50 hours.

7. Publications and Presentations

1995 Publications:

"On the Generation of a Cross Grid of Extended Screw-type Misfit Dislocations on the ZnSxSe1-x/GaAs Interface," L. H. Kuo, L. Salamanca-Riba, G. E. Hofler and B. J. Wu, Phil. Mag. **71**, 883 (1995).

"Photodegradation of CdZnSe quantum wells," G.M. Haugen, S. Guha, H. Cheng, J.M. DePuydt, M.A. Haase, G.E. Höfler, J. Qiu, and B.J. Wu, Appl. Phys. Lett. **66**, 358.

"Wide Bandgap MgZnSSe Grown on (001) GaAs by Molecular Beam Epitaxy," B. J. Wu, J. M. DePuydt, G. M. Haugen, G.E. Höfler, M.A. Haase, H. Cheng, S. Guha, J. Qiu, L. H. Kuo and L. Salamanca-Riba, Appl. Phys. Lett. **66**, 3462 (1995).

"Low-temperature process (<150°C) Ge/Pd ohmic contacts(rc ~ 10^{-6} W-cm^2) to n-type GaAs," L.C. Wang, P.H. Hao, and B.J. Wu, Appl. Phys. Lett. **67**, 509 (1995).

"Generation of degradation defects, stacking faults, and misfit dislocations in ZnSe-based films grown on GaAs," L.H. Kuo, L. Salamanca-Riba, B.J. Wu, G.M. Haugen, J.M. DePuydt, G.E. Höfler, and H. Cheng, J. Vac. Sci. Techno. **B13**, 1694 (1995).

"Low resistance (~10^6 W-cm^2) ohmic contact to n-GaAs processed at 175°C," P.H. Hao, L.C. Wang, and B.J. Wu, Electron. Lett. **31**, 1015 (1995).

"Short period superlattice II-VI blue light emitting diodes," B.J. Wu, J.M. DePuydt, G.M. Haugen, and M.A. Haase, Electron. Lett. **31**, 1015 (1995).

"Misfit strain induced tweed-twin transformation on composition modulation ZnxMg1--SySe1-y layers and the quality control of the ZnSe buffer/GaAs interface," L.H. Kuo, L. Salamanca-Riba, B.J Wu, and J.M. DePuydt, J. Electron. Mater. **24**, 155 (1995).

"Formation of screw-type misfit dislocations on the ZnSSe/GaAs interface," L.H. Kuo, L. Salamance-Riba, B.J. Wu, and G.E. Höfler, SPIE Proceedings 2346, **16** (1994).

"Transmission electron microscopy of <100> dark line defects in CdZnSe quantum well structures," G.D. Uren, G.M. Haugen, P.F. Baude, M.A. Haase, K.K. Law, T.J. Miller, and B.J. Wu, Appl. Phys. Lett. **67**, 3862 (1995).

"Dependence of the density of stacking faults in ZnSSe," L.H. Kuo, L. Salamanca-Riba, B.J. Wu, G.E. Höfler, J.M. DePuydt, and H. Cheng, Appl. Phys. Lett. **67**, 3298 (1995).

1995 Presentations:

"Defects and degradation in II-VI blue-green LEDs," S. Guha, G. M. Haugen, T. J. Miller, K. K. Law, B. J. Wu, M. A. Haase, G. D. U'Ren, invited talk at the 37th. Electronic Materials Conference, June 21-23, 1995, Charlottesville, VA.

"Blue-Green Laser Diodes for High-Density Optical Recording," P. F. Baude, T. J. Miller, G. M. Haugen, K. K. Law, and M. A. Haase, invited talk at IEEE-Intermag 95, April 17-21, 1995 Austin, TX

"Advances in Blue-Green Laser Diodes," P. F. Baude, S. Guha, M. A. Haase, G. Meis-Haugen, K. K. Law, T. J. Miller, M. Buijs, K. Haberern, T. Marshall, M. Pashley, and J. Pettruzello, invited talk at the 8th Annual IEEE Lasers and Electro-Optics Society Meeting

1996 Publications:

"Molecular beam epitaxy of low defect density (<1x10-4 cm-2) ZnSSe on GaAs," B.J. Wu, G.M. Haugen, J.M. DePuydt, L.H. Kuo and L. Salamanca-Riba, Appl. Phys. Lett. **68**, 2828 (1996).

"Conduction Band Offsets in CdZnSSe/ZnSSe Single Quantum Wells measured by Deep Level Transient Spectroscopy," P. F. Baude, M. A. Haase, G. M. Haugen, K. K. Law, T. J. Miller, K. Smekalin, J. Phillips and P. Bhattacharya, Applied Physics Letters **68**, 3591 (1996).

"Room temperature continuous-wave operation of blue-green CdZnSSe/ZnSSe quantum well laser diodes," K. K. Law, P. F. Baude, T. J. Miller, M. A. Haase, G. M. Haugen, and K. Smekalin, Electron. Lett. **32**, 345 (1996).

"Stark effect on absorption of CdZnSSe/ZnSSe Quantum Wells," K.K. Law, K. Smekalin, G.M. Haugen, G.D. Uren, and M.A. Haase, IEEE Photon. Technol. Lett. **8**, 263 (1996).

"Blue-Green Laser Diodes for Optical Data Storage," (invited) Paul Baude, Data Storage magazine, Feb. 1996

"Advances in Blue-Green Laser Diode Technology," (invited) P. F. Baude, D. C. Grillo, G. M. Haugen, K. K. Law, and T. J. Miller, IEEE-Lasers and Electro-Optics Society Newsletter, Feb. 1996

"Defect Characterization of etch pits in ZnSe based epitaxial layers," G.D. U'Ren, M.S. Goorsky, G.M. Haugen, K.K. Law, T.J. Miller and K.W. Haberern, Appl. Phys. Lett. **69** (8), 1089 (1996).

"Activation energy of Nonradiative Processes in Degraded II-VI Lasers," L.L. Chao, G.S. Cargill III, C. Kothandaraman, T. Marshall, M. Buijs, K. Haberern, J. Petruzello, G.M. Haugen, and K.K. Law, Appl. Phys. Lett. 70, p. 535 (1996)

"Growth and characterization of II-VI blue light emitting diodes using short period superlattices," B.J. Wu, L.H. Kuo, J.M. DePuydt, G.M. Haugen, M.A. Haase and L. Salamanca-Riba, Appl. Phys. Lett. 68, p. 379 (1996)

1996 Presentations:

"Blue-green II-VI Laser Diodes: Progress in Reliability," (Invited) M.A. Haase, International Symposium on Optical Data Storage and Optical Recording, Wailea, HI, July 1996.

"II-VI Blue Green Laser Diodes - Current Device Status and Understanding of Degradation Mechanisms," (Invited) G.M. Haugen et al., American Physical Society Spring Meeting, March 1996.

"II-VI Blue-Green Laser Diodes - Current Device Performance and Materials Issues," (Invited) G.M. Haugen, et al., Electrochemical Society Meeting, October 1996, Chicago, IL.

"Low-Stacking Fault density ZnSe Gowth on GaAs by Molecular Beam Epitaxy," T.J. Miller, G. M. Haugen, M. A. Haase, K. K. Law, D. C. Grillo and P. F. Baude, Electronic Materials Conference, June 26-28, 1996.

"Beryllium-Based II-VI Blue-Green Laser Diodes," T. J. Miller, P. F. Baude, G. M. Haugen, M. A. Haase, D. C. Grillo, F. R. Chien and M. D. Pashley, LEOS 1996 Conference, November 18-21, 1996, Boston, MA.

"Room Temperature CW Laser Diode at 485 nm", D.C. Grillo, P.F. Baude, T.J. Miller, K.K. Law, G.M. Haugen, F.R. Chien, M.A. Haase, M. Buijs, K.W. Haberern, and K. Shahzad, Device Research Conference, Santa Barbara, CA, June 24-26, 1996

"Recent Progress of Short Wavelength II-VI based laser diodes for optical data storage applications", P.F. Baude, et al., Workshop on II-VI Semiconductor Materials and Devices, Buffalo, NY, August 1996

SUBMITTED, IN PREPARARATION:

"Defects and degradation in wide gap II-VI based structures and light emitting devices," S. Guha, J. Petruzzello, review chapter submitted for publication to Semiconductors and Semimetals edition on II-VI widegap systems.

"Short Wavelength Room Temperature CW Laser Diodes," D. C. Grillo, P. F. Baude, T. J. Miller, G. M. Haugen, K. Smekalin, K. K. Law and M. A. Haase, in preparation for Applied Physics Letters

"Beryllium-based II-VI blue-green laser diodes," T.J. Miller, P.F. Baude, G.M. Haugen, M.A. Haase, D.C. Grillo, F.R. Chien, M. Wroge, in preparation, to be submitted to Appl. Phys. Lett.